

# Thermoelectric Properties of Multifilled Skutterudites with La as the Main Filler

HUIYUAN GENG,<sup>1,2,3</sup> TAKAHIRO OCHI,<sup>2</sup> SHOGO SUZUKI,<sup>2</sup>  
MASAAKI KIKUCHI,<sup>2</sup> SATORU ITO,<sup>2</sup> and JUNQING GUO<sup>2</sup>

1.—State Key Laboratory of Advanced Welding & Joining, Harbin Institute of Technology, Harbin 150001, China. 2.—Materials Research Laboratory, R&D Division Furukawa Co., Ltd., 1-25-13 Kannondai, Tsukuba, Ibaraki 305-0856, Japan. 3.—e-mail: genghuiyuan@hit.edu.cn

Bulk multifilled *n*- and *p*-type skutterudites with La as the main filler were fabricated using the spark plasma sintering (SPS) method. The thermoelectric properties and thermal stability of these skutterudites were investigated. It was found that the interactions among the filling atoms also play a vital role in reducing the lattice thermal conductivity of the multifilled skutterudites.  $ZT = 0.76$  for *p*-type  $\text{La}_{0.8}\text{Ba}_{0.01}\text{Ga}_{0.1}\text{Ti}_{0.1}\text{Fe}_3\text{CoSb}_{12}$  and  $ZT = 1.0$  for *n*-type  $\text{La}_{0.3}\text{Ca}_{0.1}\text{Al}_{0.1}\text{Ga}_{0.1}\text{In}_{0.2}\text{Co}_{3.75}\text{Fe}_{0.25}\text{Sb}_{12}$  skutterudites have been achieved. Furthermore, the differential scanning calorimetry (DSC) results show that there is no skutterudite phase decomposition till 750°C for the  $\text{La}_{0.8}\text{Ba}_{0.01}\text{Ga}_{0.1}\text{Ti}_{0.1}\text{Fe}_3\text{CoSb}_{12}$  sample. The thermal stability of the  $\text{La}_{0.8}\text{Ba}_{0.01}\text{Ga}_{0.1}\text{Ti}_{0.1}\text{Fe}_3\text{CoSb}_{12}$  skutterudite is greatly improved. Using the developed multifilled skutterudites, the fabricated module with size of 50 mm × 50 mm × 7.6 mm possesses maximum output power of 32 W under the condition of hot/cold sides = 600°C/50°C.

**Key words:** Skutterudite, multiple filling, thermoelectric material, thermoelectric module

## INTRODUCTION

Thermoelectric materials have attracted much attention in recent years because of their ability to directly convert heat into electricity. Among the identified thermoelectric materials, filled skutterudites<sup>1–4</sup> are considered as some of the most promising materials for commercial intermediate-temperature power generation because of their outstanding thermoelectric and mechanical properties.

The efficiency of thermoelectric materials is governed by the dimensionless figure of merit,  $ZT$ .  $ZT$  is defined as  $ZT = \alpha^2 T / \rho \kappa$ , where  $\alpha$ ,  $\rho$ ,  $\kappa$ , and  $T$  indicate the Seebeck coefficient, electrical resistivity, thermal conductivity, and absolute temperature, respectively. To further improve the  $ZT$  of filled skutterudites, double,<sup>5–8</sup> triple,<sup>9–11</sup> and multiple<sup>12</sup>

filling approaches have been proposed based on the “rattling in the oversized cage” concept. One of the main ideas of multiple filling is to use different atoms to serve as “rattlers” to scatter phonons with different frequencies. Since the Yb filling atom possesses low vibration frequency,<sup>5,13</sup> Yb is believed to be effective in scattering low-frequency phonons, which dominate the thermal conduction in crystals. Despite its high price, Yb is usually used as one of the main fillers in multifilled skutterudites, such as  $\text{Ba}_u\text{La}_v\text{Yb}_w\text{Co}_4\text{Sb}_{12}$ ,<sup>9</sup>  $\text{Ce}_{0.1}\text{In}_x\text{Yb}_y\text{Co}_4\text{Sb}_{12}$ ,<sup>10</sup>  $(\text{Sr}, \text{Ba}, \text{Yb})_y\text{Co}_4\text{Sb}_{12}$ ,<sup>11</sup> etc. In our previous work,<sup>12</sup>  $ZT = 1.0$  for *n*-type  $\text{Yb}_{0.3}\text{Ca}_{0.1}\text{Al}_{0.1}\text{Ga}_{0.1}\text{In}_{0.1}\text{Co}_{3.75}\text{Fe}_{0.25}\text{Sb}_{12}$  skutterudite was achieved. In addition,  $ZT = 0.75$  for *p*-type multifilled  $\text{La}_{0.7}\text{Ba}_{0.01}\text{Ga}_{0.1}\text{Ti}_{0.1}\text{Fe}_3\text{CoSb}_{12}$  skutterudite has also been realized. Based on the developed multifilled skutterudites, the fabricated module with size of 50 mm × 50 mm × 7.6 mm has generation performance with power output of 32 W and conversion efficiency of 8% under the condition of hot/cold sides = 600°C/50°C.

(Received July 7, 2012; accepted January 17, 2013;  
published online March 2, 2013)

However, recently the scenario of “rattling” has been challenged by neutron experimental results. Inelastic neutron scattering studies on skutterudite<sup>14</sup> and neutron triple-axis spectroscopy on clathrate<sup>15</sup> indicated that the rattlers always vibrate in a cage–rattler coupled mode. It has been argued that the rattlers do not decrease the mean free path of phonons, but lower their speed. This result indicates that there might be some drawbacks to the scenario of broad-spectrum rattler scattering. Regardless of the mechanism underlying the low thermal conductivity achieved in multifilled skutterudites, it is possible to find filling atoms other than Yb to optimize the thermoelectric properties of multifilled skutterudites.

In this paper, we report on the development of high-efficiency *n*- and *p*-type multifilled skutterudites with La as the main filler. Since La is much cheaper than Yb, the cost of the new thermoelectric materials is greatly reduced. Furthermore, the thermal stability of *p*-type skutterudite is also improved by increasing the La filling ratio from 0.7 to 0.8. The fabricated module containing the new skutterudites possesses the same generation performance as the previous module using Yb as the main filling atom.

## EXPERIMENTAL PROCEDURES

### Synthesis Procedures

High-purity metals of 99.999% Sb, 99.9% Co, Fe, La, Yb, Ce, Al, Ga, In, and Ti, and 99% Ba and Ca were used as starting materials to synthesize the *p*- and *n*-type skutterudite samples. A total amount of 20 g of stoichiometric starting materials were first loaded into carbon crucibles, which were further sealed in quartz tubes under vacuum ( $<10^{-3}$  Pa). Then, the quartz tubes were transferred to a programmable furnace. After holding at 1150°C for 12 h, the quartz tubes were quenched in cold water (about 25°C). Subsequently, the water-quenched samples were annealed at 700°C for another 100 h. Finally, all of each annealed sample was ground into fine powder (below 150  $\mu\text{m}$ ) and densified by the SPS method at temperature of 700°C under pressure of 60 MPa.

### Characterization Procedures

The distribution of filling atoms in the SPS samples was examined by energy-dispersive x-ray spectroscopy (EDX) mapping using a Horiba Emax-7000 probe attached to a Hitachi S4700 scanning electronic microscope (SEM).

A round disk with diameter of 10 mm and a bar (2 mm  $\times$  2 mm  $\times$  18 mm) were cut from the same SPS sample. The Seebeck coefficient and electrical resistivity were measured simultaneously on the bar by the standard four-probe method (ULVAC-Riko, ZEM-2) from room temperature to 600°C under helium atmosphere.

The thermal diffusivity from room temperature to 600°C of the synthesized samples was determined on the disk by a laser flash method (ULVAC-Riko, TC-7000). The specific heat capacity was measured by a high-precision, reliable DSC method (NET-ZSCH DSC404c). The thermal conductivity is the product of the thermal diffusivity, the specific heat capacity, and the density of the sample. The lattice thermal conductivity ( $\kappa_L$ ) was then obtained by subtracting the electron thermal conductivity from the total thermal conductivity using the Wiedemann–Franz law with a Lorenz number of  $2.0 \times 10^{-8}$  W  $\Omega$  K<sup>-2</sup>.

## RESULTS AND DISCUSSION

### Thermoelectric Properties of the *n*-Type Multifilled Skutterudites

It was found in our previous work<sup>12</sup> that *n*-type multifilled  $\text{Yb}_{0.3}\text{Ca}_{0.1}\text{Al}_{0.1}\text{Ga}_{0.1}\text{In}_{0.1}\text{Co}_{3.75}\text{Fe}_{0.25}\text{Sb}_{12}$

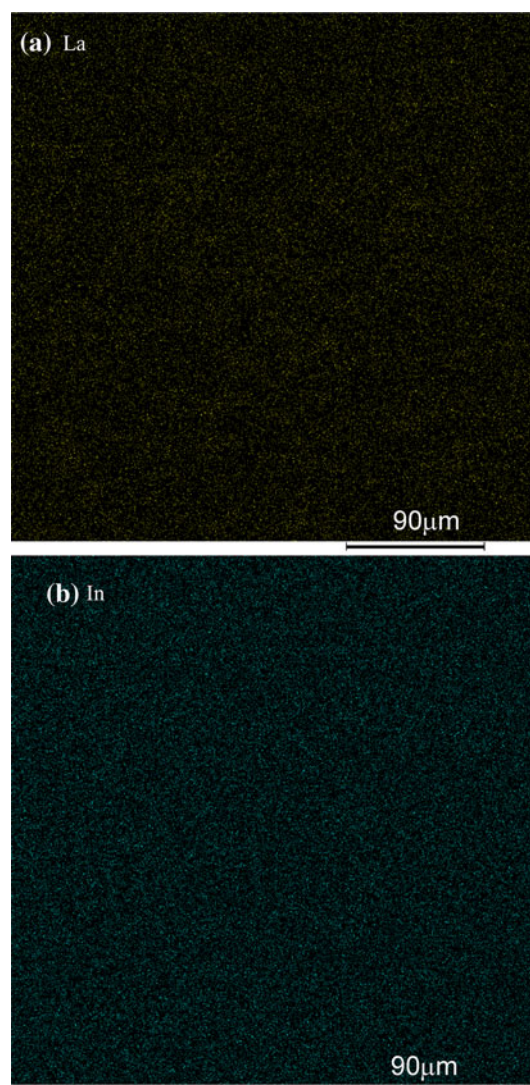
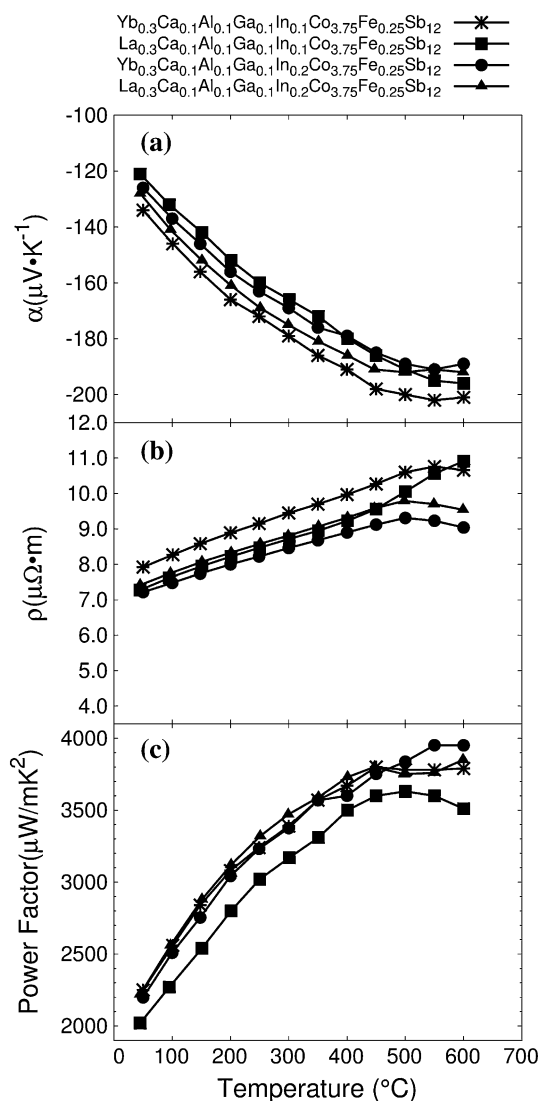
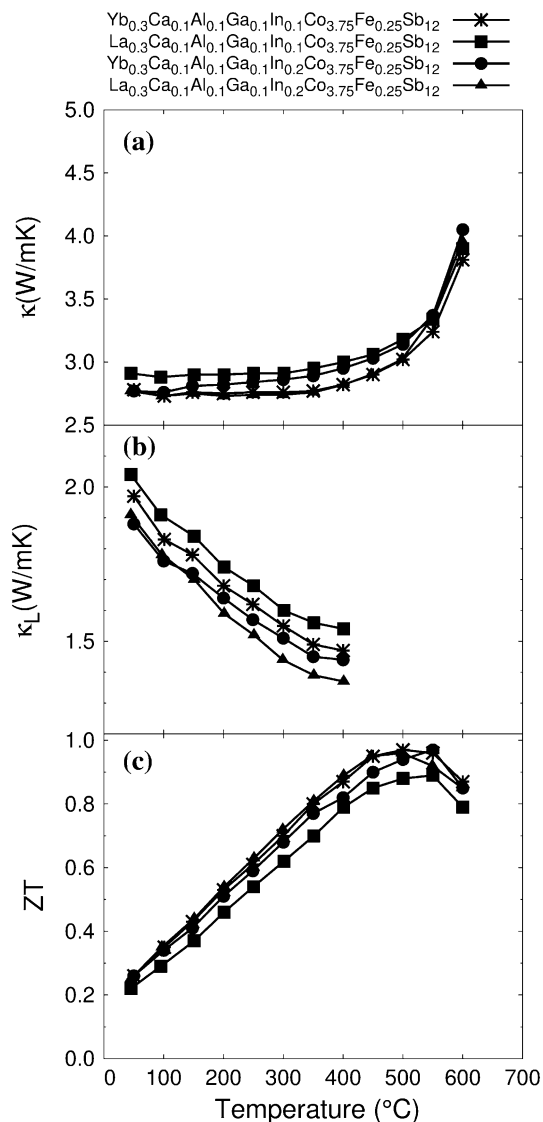


Fig. 1. EDX mapping of the filling atoms in the  $\text{La}_{0.3}\text{Ca}_{0.1}\text{Al}_{0.1}\text{Ga}_{0.1}\text{In}_{0.1}\text{Co}_{3.75}\text{Fe}_{0.25}\text{Sb}_{12}$  skutterudite: (a) La, and (b) In.

**Table I. Nominal and actual composition of the multifilled skutterudites as measured by ICP-AES**

Nominal	Actual
$\text{La}_{0.3}\text{Ca}_{0.1}\text{Al}_{0.1}\text{Ga}_{0.1}\text{In}_{0.2}\text{Co}_{3.75}\text{Fe}_{0.25}\text{Sb}_{12}$	$\text{La}_{0.33}\text{Ca}_{0.09}\text{Al}_{0.07}\text{Ga}_{0.1}\text{In}_{0.22}\text{Co}_{3.75}\text{Fe}_{0.28}\text{Sb}_{11.6}$
$\text{La}_{0.8}\text{Ba}_{0.01}\text{Ga}_{0.1}\text{Ti}_{0.1}\text{Fe}_3\text{CoSb}_{12}$	$\text{La}_{0.8}\text{Ba}_{0.01}\text{Ga}_{0.1}\text{Ti}_{0.07}\text{Fe}_{3.1}\text{CoSb}_{12.3}$

Fig. 2. Temperature dependence of (a) the Seebeck coefficient, (b) the electrical resistivity, and (c) the power factor for the *n*-type multifilled skutterudites.Fig. 3. Temperature dependence of (a) the total thermal conductivity, (b) the lattice thermal conductivity, and (c) the dimensionless figure of merit for the *n*-type multifilled skutterudites.

skutterudite possesses relative high  $ZT$  of 1.0. So, this material is used as the reference material to study the effects of La filling on the thermoelectric properties of *n*-type multifilled skutterudites.

According to the SEM results (not shown), no secondary phases were found in the grain boundaries. All of the filling atoms were evenly distributed in the SPS samples. Figure 1 shows EDX mapping results for the filling atoms in the  $\text{La}_{0.3}\text{Ca}_{0.1}\text{Al}_{0.1}\text{Ga}_{0.1}\text{In}_{0.2}\text{Co}_{3.75}\text{Fe}_{0.25}\text{Sb}_{12}$  skutterudite. The actual

composition of this sample was also analyzed by inductively coupled plasma-atomic emission spectrometry (ICP-AES), as listed in Table I.

Figure 2 shows the Seebeck coefficient and electrical resistivity of the *n*-type multifilled skutterudites with La as the main filler. For the  $\text{La}_{0.3}\text{Ca}_{0.1}\text{Al}_{0.1}\text{Ga}_{0.1}\text{In}_{0.2}\text{Co}_{3.75}\text{Fe}_{0.25}\text{Sb}_{12}$  skutterudite, by simply switching the main filler from Yb with filling ratio of 0.3 to La with filling ratio of 0.3,

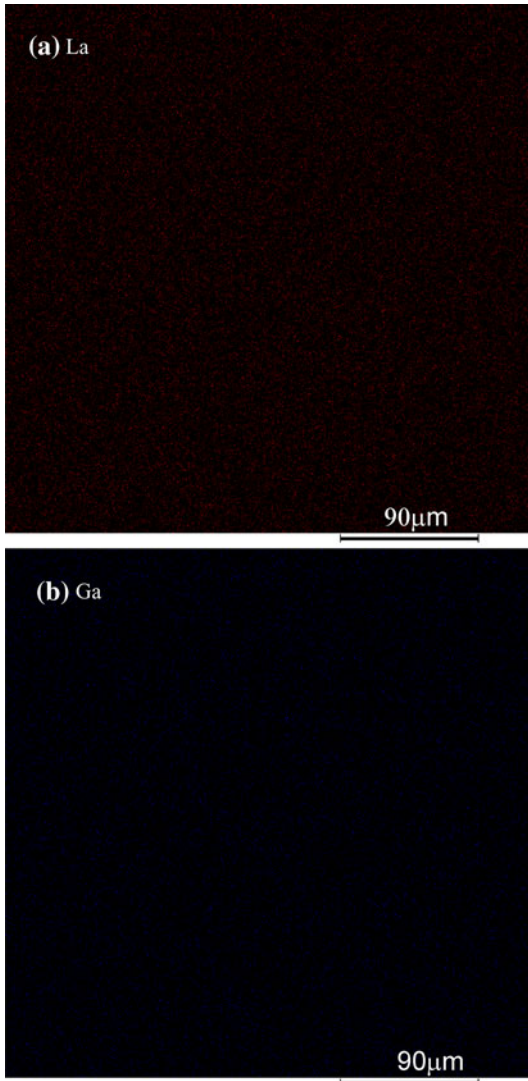


Fig. 4. EDX mapping of the filling atoms in the  $\text{La}_{0.8}\text{Ba}_{0.01}\text{Ga}_{0.1}\text{Ti}_{0.1}\text{Fe}_3\text{CoSb}_{12}$  skutterudite: (a) La, and (b) Ga.

both the Seebeck coefficient and electrical resistivity are reduced. Since the ion charge of La is +3 while it is +2 for Yb,<sup>1,16</sup> the reduction of the Seebeck coefficient and electrical resistivity is considered to be caused by an increase in the carrier concentration.

According to Fig. 2c, the power factor of the  $\text{La}_{0.3}\text{Ca}_{0.1}\text{Al}_{0.1}\text{Ga}_{0.1}\text{In}_{0.1}\text{Co}_{3.75}\text{Fe}_{0.25}\text{Sb}_{12}$  skutterudite is lower than that of the  $\text{Yb}_{0.3}\text{Ca}_{0.1}\text{Al}_{0.1}\text{Ga}_{0.1}\text{In}_{0.1}\text{Co}_{3.75}\text{Fe}_{0.25}\text{Sb}_{12}$  skutterudite by about 5%. What is worse, the introduction of La increases the thermal conductivity of  $\text{La}_{0.3}\text{Ca}_{0.1}\text{Al}_{0.1}\text{Ga}_{0.1}\text{In}_{0.1}\text{Co}_{3.75}\text{Fe}_{0.25}\text{Sb}_{12}$  skutterudite, as shown in Fig. 3a. Therefore, the reduced power factor and increased thermal conductivity result in a decreased dimensionless figures of merit of  $ZT = 0.9$  for the  $\text{La}_{0.3}\text{Ca}_{0.1}\text{Al}_{0.1}\text{Ga}_{0.1}\text{In}_{0.1}\text{Co}_{3.75}\text{Fe}_{0.25}\text{Sb}_{12}$  skutterudite, as shown in Fig. 3c.

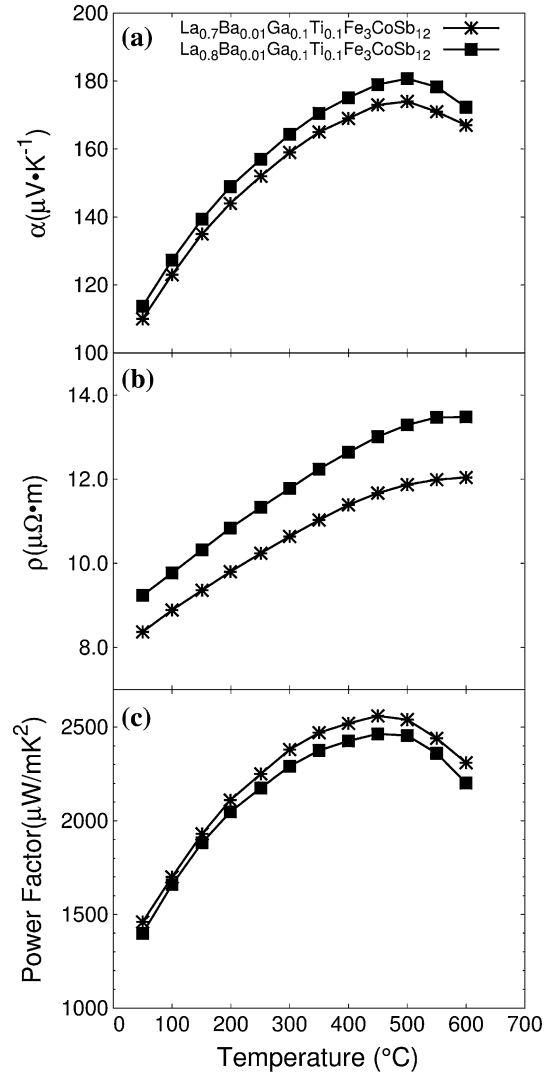


Fig. 5. Temperature dependence of (a) the Seebeck coefficient, (b) the electrical resistivity, and (c) the power factor for the *p*-type multifilled skutterudites.

On the other hand, the increase of the In filling ratio from 0.1 to 0.2 results in an improved  $ZT$  for the  $\text{La}_{0.3}\text{Ca}_{0.1}\text{Al}_{0.1}\text{Ga}_{0.1}\text{In}_{0.2}\text{Co}_{3.75}\text{Fe}_{0.25}\text{Sb}_{12}$  skutterudite, as shown in Figs. 2 and 3. Compared with the  $\text{La}_{0.3}\text{Ca}_{0.1}\text{Al}_{0.1}\text{Ga}_{0.1}\text{In}_{0.1}\text{Co}_{3.75}\text{Fe}_{0.25}\text{Sb}_{12}$  skutterudite, the increased filling ratio of In increases the Seebeck coefficient and electrical resistivity, resulting in a higher power factor. The power factor of the  $\text{La}_{0.3}\text{Ca}_{0.1}\text{Al}_{0.1}\text{Ga}_{0.1}\text{In}_{0.2}\text{Co}_{3.75}\text{Fe}_{0.25}\text{Sb}_{12}$  skutterudite is also comparable to that of the  $\text{Yb}_{0.3}\text{Ca}_{0.1}\text{Al}_{0.1}\text{Ga}_{0.1}\text{In}_{0.1}\text{Co}_{3.75}\text{Fe}_{0.25}\text{Sb}_{12}$  reference sample.

Most interestingly, a low lattice thermal conductivity is also achieved by increasing the In filling ratio from 0.1 to 0.2 in the  $\text{La}_{0.3}\text{Ca}_{0.1}\text{Al}_{0.1}\text{Ga}_{0.1}\text{In}_{0.2}\text{Co}_{3.75}\text{Fe}_{0.25}\text{Sb}_{12}$  skutterudite, as shown in Fig. 3b. The lattice thermal conductivity of the  $\text{La}_{0.3}\text{Ca}_{0.1}\text{Al}_{0.1}\text{Ga}_{0.1}\text{In}_{0.2}\text{Co}_{3.75}\text{Fe}_{0.25}\text{Sb}_{12}$  skutterudite at 400°C is 1.37 W/mK, which is very close to the

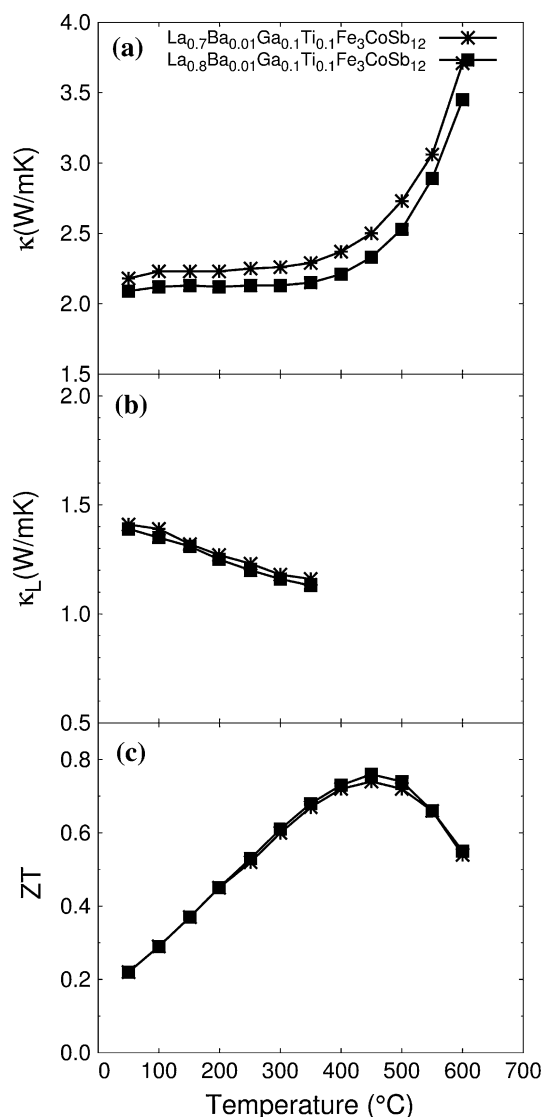


Fig. 6. Temperature dependence of (a) the total thermal conductivity, (b) the lattice thermal conductivity, and (c) the dimensionless figure of merit for the  $\rho$ -type multifilled skutterudites.

lattice thermal conductivity of the  $\text{Yb}_{0.3}\text{Ca}_{0.1}\text{Al}_{0.1}\text{Ga}_{0.1}\text{In}_{0.1}\text{Co}_{3.75}\text{Fe}_{0.25}\text{Sb}_{12}$  reference sample.

The electron thermal conductivity of the  $\text{La}_{0.3}\text{Ca}_{0.1}\text{Al}_{0.1}\text{Ga}_{0.1}\text{In}_{0.2}\text{Co}_{3.75}\text{Fe}_{0.25}\text{Sb}_{12}$  skutterudite is slightly higher than that of the  $\text{Yb}_{0.3}\text{Ca}_{0.1}\text{Al}_{0.1}\text{Ga}_{0.1}\text{In}_{0.1}\text{Co}_{3.75}\text{Fe}_{0.25}\text{Sb}_{12}$  reference sample, but the total thermal conductivities of both samples are quite similar over the whole measuring temperature range. As a result, a ZT of about 1.0 is achieved in the  $\text{La}_{0.3}\text{Ca}_{0.1}\text{Al}_{0.1}\text{Ga}_{0.1}\text{In}_{0.2}\text{Co}_{3.75}\text{Fe}_{0.25}\text{Sb}_{12}$  skutterudite at 500  $^{\circ}\text{C}$ . Considering that La is much cheaper than Yb, the  $\text{La}_{0.3}\text{Ca}_{0.1}\text{Al}_{0.1}\text{Ga}_{0.1}\text{In}_{0.2}\text{Co}_{3.75}\text{Fe}_{0.25}\text{Sb}_{12}$  skutterudite is advantageous for commercial thermoelectric applications. In the current work, a significant cost saving for the filling elements can be achieved by substituting La for Yb.

Furthermore, to clarify the role of the In filling atoms, a  $\text{Yb}_{0.3}\text{Ca}_{0.1}\text{Al}_{0.1}\text{Ga}_{0.1}\text{In}_{0.2}\text{Co}_{3.75}\text{Fe}_{0.25}\text{Sb}_{12}$

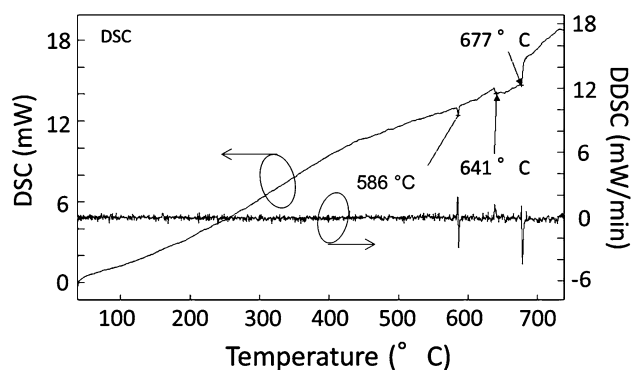


Fig. 7. Temperature-dependent DSC curve of the  $\text{La}_{0.7}\text{Ba}_{0.01}\text{Ga}_{0.1}\text{Ti}_{0.1}\text{Fe}_3\text{CoSb}_{12}$  skutterudite.

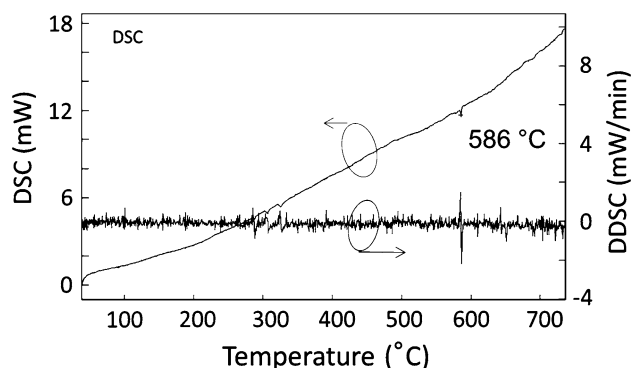


Fig. 8. Temperature-dependent DSC curve of the  $\text{La}_{0.8}\text{Ba}_{0.01}\text{Ga}_{0.1}\text{Ti}_{0.1}\text{Fe}_3\text{CoSb}_{12}$  skutterudite.

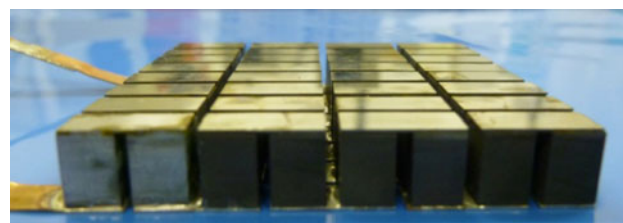


Fig. 9. Thermoelectric generator module containing the newly developed multifilled skutterudites with La as the main filler.

skutterudite sample was also synthesized. Unlike the multifilled skutterudites with La as the main filler, increase of the In filling ratio from 0.1 to 0.2 did not greatly affect the lattice thermal conductivity in the multifilled skutterudites with Yb as the main filler. The lattice thermal conductivity of the  $\text{Yb}_{0.3}\text{Ca}_{0.1}\text{Al}_{0.1}\text{Ga}_{0.1}\text{In}_{0.2}\text{Co}_{3.75}\text{Fe}_{0.25}\text{Sb}_{12}$  skutterudite at 400  $^{\circ}\text{C}$  is 1.44  $\text{W/mK}$ , as shown in Fig. 3b.

Since the vibration frequency of the La atom in the filled skutterudite is believed to be higher than that of the Yb atom according to the “rattling” theory,<sup>5</sup> La is considered to be less effective in reducing the lattice thermal conductivity in the filled skutterudites. Our current results indicate that interactions among filling atoms also play a vital role in reducing the lattice thermal conductivity of the multifilled skutterudites. Therefore, a

**Table II. Power generation performance of the module**

<i>n</i> -Type material	$\text{La}_{0.3}\text{Ca}_{0.1}\text{Al}_{0.1}\text{Ga}_{0.1}\text{In}_{0.2}\text{Co}_{3.75}\text{Fe}_{0.25}\text{Sb}_{12}$
<i>p</i> -Type material	$\text{La}_{0.8}\text{Ba}_{0.01}\text{Ga}_{0.1}\text{Ti}_{0.1}\text{Fe}_3\text{CoSb}_{12}$
Open-circuit voltage	4.92 V
Maximum output power	32 W
Voltage at maximum power	2.46 V
Current at maximum power	13A

competitive low lattice thermal conductivity was also achieved in the  $\text{La}_{0.3}\text{Ca}_{0.1}\text{Al}_{0.1}\text{Ga}_{0.1}\text{In}_{0.2}\text{Co}_{3.75}\text{Fe}_{0.25}\text{Sb}_{12}$  skutterudite.

### Thermoelectric Properties and Thermal Stability of the *p*-Type Multifilled Skutterudites

Skutterudite-based thermoelectric generators are expected to work at hot-side temperatures of over 600°C. Therefore, the thermal stability of the multifilled skutterudites is quite critical, especially for the low-melting-point *p*-type skutterudites. In our previous work, a *p*-type  $\text{La}_{0.7}\text{Ba}_{0.01}\text{Ga}_{0.1}\text{Ti}_{0.1}\text{Fe}_3\text{CoSb}_{12}$  multifilled skutterudite was developed. To further improve its thermal stability, the effects of the La filling ratio were studied in the current work.

As for the *n*-type skutterudites, all of these filling atoms were evenly distributed in the SPS samples, and no secondary phases were found in the grain boundaries under SEM observation. Figure 4 shows EDX mapping of the filling atoms in the  $\text{La}_{0.8}\text{Ba}_{0.01}\text{Ga}_{0.1}\text{Ti}_{0.1}\text{Fe}_3\text{CoSb}_{12}$  skutterudite. The actual composition of this sample as measured by ICP-AES is also given in Table I.

Figure 5 shows the electrical properties of the  $\text{La}_{0.7}\text{Ba}_{0.01}\text{Ga}_{0.1}\text{Ti}_{0.1}\text{Fe}_3\text{CoSb}_{12}$  and  $\text{La}_{0.8}\text{Ba}_{0.01}\text{Ga}_{0.1}\text{Ti}_{0.1}\text{Fe}_3\text{CoSb}_{12}$  multifilled skutterudites. By increasing the La filling ratio from 0.7 to 0.8 in the skutterudites, both the Seebeck coefficient and electrical resistivity increase owing to the decreased carrier concentration. As a result, the power factor of the  $\text{La}_{0.8}\text{Ba}_{0.01}\text{Ga}_{0.1}\text{Ti}_{0.1}\text{Fe}_3\text{CoSb}_{12}$  skutterudite is about 96% of that of the  $\text{La}_{0.7}\text{Ba}_{0.01}\text{Ga}_{0.1}\text{Ti}_{0.1}\text{Fe}_3\text{CoSb}_{12}$  skutterudite (at 450°C), as shown in Fig. 5c.

On the other hand, both the electron and lattice thermal conductivities of the  $\text{La}_{0.8}\text{Ba}_{0.01}\text{Ga}_{0.1}\text{Ti}_{0.1}\text{Fe}_3\text{CoSb}_{12}$  skutterudite are reduced by the increased La concentration, as shown in Fig. 6. The total thermal conductivity of the  $\text{La}_{0.8}\text{Ba}_{0.01}\text{Ga}_{0.1}\text{Ti}_{0.1}\text{Fe}_3\text{CoSb}_{12}$  skutterudite is about 93% of that of the  $\text{La}_{0.7}\text{Ba}_{0.01}\text{Ga}_{0.1}\text{Ti}_{0.1}\text{Fe}_3\text{CoSb}_{12}$  skutterudite (at 450°C), as shown in Fig. 6a. Therefore, a *ZT* of 0.76 for the  $\text{La}_{0.8}\text{Ba}_{0.01}\text{Ga}_{0.1}\text{Ti}_{0.1}\text{Fe}_3\text{CoSb}_{12}$  skutterudite is realized at 450°C, as shown in Fig. 6c.

Figure 7 shows the DSC curve of the  $\text{La}_{0.7}\text{Ba}_{0.01}\text{Ga}_{0.1}\text{Ti}_{0.1}\text{Fe}_3\text{CoSb}_{12}$  skutterudite. The peak at about 596°C represents the skutterudite–Sb eutectic

point, because there is always some trace amount of Sb in the as-sintered sample. Another broad peak between 641°C and 677°C represents the decomposition of the skutterudite phase. Such a low decomposition temperature should be avoided from the application point of view.

On the contrary, Fig. 8 shows that the broad peak disappears over the whole measuring temperature range (under 750°C) for the  $\text{La}_{0.8}\text{Ba}_{0.01}\text{Ga}_{0.1}\text{Ti}_{0.1}\text{Fe}_3\text{CoSb}_{12}$  skutterudite, indicating remarkably improved thermal stability. The reason for this improvement will be studied in future work.

### Power Generation Performance of the Thermoelectric Module

Using the technologies described in Ref. 12, a thermoelectric generator module containing the newly developed multifilled skutterudites with La as the main filler was successfully developed, as shown in Fig. 9. The module is made from several 20-g ingots. All of these ingots possess similar room-temperature transport properties. The module with size of 50 mm × 50 mm × 7.6 mm consists of 32 pairs of *p/n* elements with element size of 5 mm × 5 mm × 7.6 mm. Details of the module measurement apparatus can be found in Ref. 17. Under the condition of hot/cold sides = 600°C/50°C, the maximum output power generation is 32 W, the same as that of the previous module using Yb as the main filler. Table II lists the detailed power generation performance of the module.

### CONCLUSIONS

*ZT* = 0.76 for *p*-type  $\text{La}_{0.8}\text{Ba}_{0.01}\text{Ga}_{0.1}\text{Ti}_{0.1}\text{Fe}_3\text{CoSb}_{12}$  and *ZT* = 1.0 for *n*-type  $\text{La}_{0.3}\text{Ca}_{0.1}\text{Al}_{0.1}\text{Ga}_{0.1}\text{In}_{0.2}\text{Co}_{3.75}\text{Fe}_{0.25}\text{Sb}_{12}$  skutterudites with La as the main filler have been realized. Furthermore, the thermal stability of the  $\text{La}_{0.8}\text{Ba}_{0.01}\text{Ga}_{0.1}\text{Ti}_{0.1}\text{Fe}_3\text{CoSb}_{12}$  skutterudite is greatly improved compared with that of the  $\text{La}_{0.7}\text{Ba}_{0.01}\text{Ga}_{0.1}\text{Ti}_{0.1}\text{Fe}_3\text{CoSb}_{12}$  skutterudite. The fabricated module with size of 50 mm × 50 mm × 7.6 mm has generation performance with power output of 32 W under the condition of hot/cold sides = 600°C/50°C.

### REFERENCES

1. G.A. Slack, *CRC Handbook of Thermoelectrics*, ed. D.M. Rowe (Boca Raton, FL: CRC Press, 1995), pp. 407–440.
2. G.S. Nolas, M. Kaeser, R.T. Littleton IV, and T.M. Tritt, *Appl. Phys. Lett.* 77, 1855 (2000).
3. Y.G. Wang, X.F. Xu, and J.H. Yang, *Phys. Rev. Lett.* 102, 175508 (2009).
4. H.Y. Geng, S. Ochi, and J.Q. Guo, *Appl. Phys. Lett.* 91, 022106 (2007).
5. J. Yang, W. Zhang, S.Q. Bai, Z. Mei, and L.D. Chen, *Appl. Phys. Lett.* 90, 192111 (2007).
6. X. Shi, H. Kong, C.P. Li, C. Uher, J. Yang, J.R. Salvador, H. Wang, L. Chen, and W. Zhang, *Appl. Phys. Lett.* 92, 182101 (2008).

7. W.Y. Zhao, P. Wei, Q.J. Zhang, C.L. Dong, L.S. Liu, and X.F. Tang, *J. Am. Chem. Soc.* 131, 3713 (2009).
8. J.Y. Peng, J. He, Z. Su, P.N. Alboni, S. Zhu, and T.M. Tritt, *J. Appl. Phys.* 105, 084907 (2009).
9. X. Shi, J. Yang, J.R. Salvador, M.F. Chi, J.Y. Cho, H. Wang, S.Q. Bai, J.H. Yang, W.Q. Zhang, and L.D. Chen, *J. Am. Chem. Soc.* 133, 7837 (2011).
10. J. Graff, S. Zhu, T. Holgate, J.Y. Peng, J. He, and T.M. Tritt, *J. Electron. Mater.* 40, 696 (2011).
11. L. Zhang, A. Grytsiv, P. Rogl, E. Bauer, and M. Zehetbauer, *J. Phys. D* 42, 225405 (2009).
12. J.Q. Guo, H.Y. Geng, T. Ochi, S. Suzuki, M. Kikuchi, and S. Ito, *J. Electron. Mater.* 41, 1036 (2012).
13. I.K. Dimitrov, M.E. Manley, S.M. Shapiro, J. Yang, W. Zhang, L.D. Chen, Q. Jie, G. Ehlers, A. Podlesnyak, J. Camacho, and Q. Li, *Phys. Rev. B* 82, 174301 (2010).
14. M.M. Koza, M.R. Johnson, R. Viennois, H. Girard, and D. Ravot, *Nat. Mater.* 7, 805 (2008).
15. M. Christensen, A.B. Abrahamsen, N.B. Christensen, F. Juranyi, N.H. Andersen, K. Lefmann, J. Andreasson, C.R.H. Bahl, and B.B. Iversen, *Nat. Mater.* 7, 811 (2008).
16. G.S. Nolas, D.T. Morelli, and T.M. Tritt, *Annu. Rev. Mater. Sci.* 29, 89 (1999).
17. H. Takazawa, H. Obara, Y. Okada, K. Kobayashi, T. Onishi, and T. Kajikawa, *Proceedings of the 25th International Conference on Thermoelectrics* (IEEE, Piscataway, 2006).